An Input-voltage-sharing Control Strategy of Input-series-output-parallel Isolated Bidirectional DC/DC Converter for DC Distribution Network

Yu Wang, *Member IEEE*, Yuanpeng Guan, Olav Bjarte Fosso, *Senior Member IEEE*, Marta Molinas, *Member IEEE*, Si-Zhe Chen and Yun Zhang

***Abstract* — Input-series-output-parallel (ISOP) isolated bidirectional DC/DC converter (IBDC) become a preferred scheme connecting high-voltage and low-voltage bus in DC distribution network. Input-voltage-sharing (IVS) among modules is essential to realize the stable operation of ISOP system. Nowadays, with large-scale access of distributed energy sources and loads in DC grids, the fluctuations in bus voltage and connected load become frequent and great, deteriorating the IVS performance and stable operation of ISOP structure IBDC. To solve this issue, a triple-close-loop IVS strategy is proposed in this paper. Compared with conventional IVS strategy with constant input impedance, the proposed IVS strategy reshapes input impedance to be a full-order model containing high-order components and sensitive to fluctuation of output voltage, and IVS control based on reshaped impedance improves dynamics feature, maintains ideal output power and avoids false protection and potential instability for ISOP structure IBDC under frequent and large fluctuation. Experimental results verify correctness and effectiveness of the analysis and proposed strategy, providing a feasible,efficient and practical control scheme for ISOP system in DC distribution network.**

***Index Terms* — DC distribution network, ISOP structure IBDC, input voltage sharing control strategy, dynamics and stability characteristics.**

I. Introduction

With the rapid development of distributed renewable power sources, energy storage device and direct-current (DC) equipment, the DC distribution networks have been significantly attracting global attentions and became important elements for future power systems [1]-[2]. Compared with conventional alternating-current (AC) distribution network, the DC distribution network obtains higher power conversion efficiency, flexible access to renewable energy and devices, avoid synchronization and reactive power compensation issues, effectively reduce power converter, power consumption and construction cost [3]-[4]. The common structure of DC distribution network is presented in Fig. 1. Nowadays, the research and development on DC distribution networks not only focus on low-voltage DC (LVDC) but also extend to medium-voltage DC (MVDC) and high-voltage DC (HVDC), and many projects are completed or under construction, such as Gotland project in Sweden, Tj Reborg project in Denmark and Zhoushan DC transmission project in China [5]-[6].

The high-frequency isolated bidirectional DC converter (IBDC) with advantages of low volume and cost, light weight, low conversion noise, high power density and efficiency plays an important role in buses connection, voltage conversion, power transmission and electrical isolation in DC distribution networks [7]-[8]. Among the various topologies of IBDC, the dual-active-bridge (DAB) is considered to be a basic topology and attracts attentions from engineers and researchers [9]-[10]. However, due to limitation in manufacturing of semiconductor devices, a single DAB cannot satisfy the voltage and power requirements in MVDC and HVDC applications. To increase the voltage, current and power ratings, the IBDC based on modular multilevel converter (MDCC) topology was proposed. However, topology, corresponding control and implementation process of MDCC containing sub-modules are complicated, and the high-frequency transformers with such high voltage and power ratings in MDCC are not feasible to produce for satisfying the MVDC and HVDC practical requirements, thus hindering the application of MDCC [11]-[12].

To increase voltage and power ratings, the multiple modular IBDC scheme including the input-series-output-parallel (ISOP), input-series-output-series (ISOS), input-parallel-output-series (IPOS) and input-parallel-output-parallel (IPOP) structures provide alternative schemes [13]-[15]. Compared with MDCC scheme, the multiple modular IBDC scheme obtains modular and redundant architecture, flexible and reliable installation and control structure, higher power transmission capability option, with lower reactive power smaller current stress, becoming a preferred IBDC solution for MVDC and HVDC networks [16].

Manuscript received June 16, 2021; accepted August 19, 2021. This work was supported by National Natural Science Foundation of China under grant No. 61802070, and Natural Science Foundation of Guangdong Province under grant No. 2020A1515010766 and 2021A1515012398, and the Project of State Key Laboratory of Power System and Generation Equipment under grant No. SKLD20M21. (*Corresponding author: Yuanpeng Guan*)

Y. Wang, S. Z. Chen and Y. Zhang are with the School of Automation, Guangdong University of Technology, Guangzhou 510006, China (e-mail: yuwang@gdut.edu.cn; sizhe.chen@gdut.edu.cn; yun@gdut.edu.cn)

Y. Guan is with the Energy Electricity Research Center, Jinan University, Zhuhai 519070, China (e-mail: guanyuanpeng@126.com).

O. B. Fosso is with Department of Electric Power Engineering, Norwegian University of Science and Technology, Trondheim 7491, Norway (e-mail: olav.fosso@ntnu.no).

M. Molinas is with the Department of Engineering Cybernetics, Norwegian University of Science and Technology, Trondheim 7491, Norway (e-mail: marta.molinas@ntnu.no).

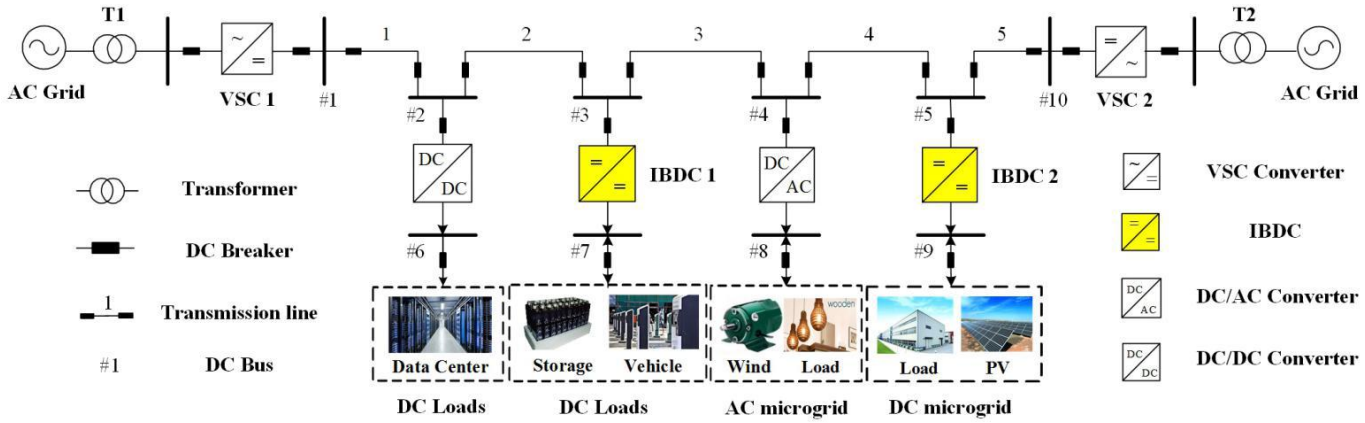

Fig. 1. The system structure of DC distribution network.

Among multiple modular IBDCs, ISOP configuration suitable for high input-voltage and large output-current application attracts a growing attention in recent years. Generally, the input-voltage-sharing (IVS) and output-current-sharing (OCS) among modules must be guaranteed to realize stable operation of ISOP system, and based on principle of power conversion, the IVS means OCS, and vice versa [17]-[18].

To achieve power sharing among modules, many strategies have been investigated, which can be mainly classified into two categories: the natural voltage and current sharing methods without special controller, and the equilibrium methods with specific IVS and OCS controllers [19]-[20]. For the natural voltage and current sharing method such as common-duty-ratio control strategy depends on self-regulating and without specific IVS or OCS controllers, control structure and implementation are simple. However, it is difficult to achieve IVS and OCS due to the inevitable parameter mismatches among modules in practice. Besides, the steady-state and dynamic characteristics of the system are poor [21]-[22]. Therefore, to achieve exact sharing of input voltage and output current, control methods with dedicated IVS or OCS controllers can be applied. On one hand, input voltage feed-forward control scheme with various inner current control loops are usually applied to realize the IVS for ISOP systems, obtaining the ability to suppress input bus perturbations and good dynamic characteristics [23]-[25]. In addition, the information of output currents of constituent modules can also be employed to realize the OCS for ISOP systems. These specific control strategies can not only achieve the excellent power balance, but also improve the dynamic and steady-state performance [26]-[27]. However, the modules in ISOP structure IBDC still share the same central controller, limiting the benefit of modularity, reliability and expansibility. Moreover, the ISOP system tends to collapse once the central controller or common control loop is malfunctioning.

To solve the problem, the decentralized IVS or OCS control strategies for ISOP system, such as input voltage droop control and output current inverse droop control, were proposed to achieve the power sharing [28]-[30]. The decentralized strategy realizes IVS and OCS and also has advantages of no control interconnection and communication among modules. However, these control strategies mainly concern the output voltage and current control, the interaction and influence from IVS or OCS control loop on the performance of ISOP system have not been discussed in detail. Thus, these control strategies do not have ideal dynamic characteristics, and the output voltage suffers from the input voltages unbalances and interaction between parallel output ports, leading to potential instability especially when the range of input voltage is wide [31]-[32]. Moreover, some existing studies realize IVS for ISOP structure IBDC by reshaping the input impedance with a small-signal positive virtual input impedance. However, the ideal constant resistance is usually used to represent the input impedance, and it's difficult to reflect dynamic characteristics of input variables. Besides, its input impedance analysis and controller design for module often ignores higher-order components, hindering the precise and rapid control and leading to potential instability for ISOP structure IBDC [33]-[35]. Nowadays, with the large-scale access of distributed energy sources and variety of loads in DC distribution networks, the fluctuation of DC bus voltages and connected loads become more frequent and larger, and the performance of ISOP structure IBDC under conventional IVS strategy may be deteriorated, leading to the unexpected false protection activation and potential instability, especially in high-voltage application scenarios [36].

To overcome above mentioned limitations, a triple-close-loop IVS control strategy is proposed for ISOP structure IBDC in this paper. By adding current control loops to conventional IVS strategy, the proposed IVS strategy realizes ideal IVS and decouple operation and avoids communication among modules, maintaining the modularity and reliability for ISOP system. Besides, the proposed IVS strategy reshapes input impedance, and the full-order mathematical model of ISOP structure IBDC with high-order components is established. The proposed IVS controller designed with reshaped impedance is sensitive to the fluctuation of output voltage, improving dynamic characteristic, maintaining ideal output power and avoiding false protection activation and potential instability for ISOP structure IBDC under the frequent and large fluctuations in connected loads and DC buses voltage, making it a feasible, efficient and practical control scheme for ISOP structure IBDC, especially applied in DC distribution network with large-scale access of distributed sources and diverse loads.

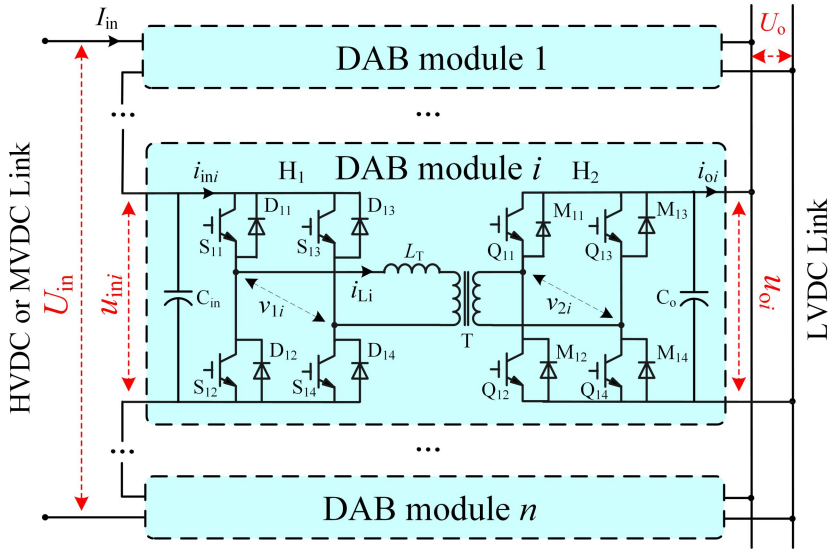

Fig. 2. The ISOP structure IBDC scheme based on DAB modules.

II. Topology Configuration and Mathematical Model of ISOP Structure IBDC

To present the analysis and proposed control strategy for multiple modular IBDC scheme, the ISOP structure IBDC based on DAB converters is studied, as shown in Fig. 2. Each DAB module is a symmetric topology composed of two full-bridges H_1 and H_2, a high-frequency isolated transformer with voltage ratio n_T and an auxiliary inductance L_T. On the HVDC or MVDC side, n DAB modules are connected in series to increase voltage rating. On the LVDC side, n DAB modules are connected in parallel to increase the current level. C_{in} and C_o are the capacitance on primary and secondary sides of multiple modular IBDC, respectively. U_{in}, U_o, I_{in} and I_o are DC voltages and currents on the primary and secondary sides of IBDC, respectively. u_{ini}, u_{oi}, i_{ini} and i_{oi} are DC voltages and currents on primary and secondary sides of DAB module, and v_{1i}, v_{2i} and i_{Li} are high-frequency-link (HFL) voltages and current in DAB module, respectively. The power conversion of each DAB can be viewed as power exchange between equivalent HFL voltage source v_{1i} and v_{2i} through equivalent inductor L_T. The HFL current i_{Li} can be varied by adjusting the phase-shift D between HFL voltages v_{1i} and v_{2i}, controlling the power rating and power direction for DAB module and multiple modular IBDC.

From the ISOP configuration of multiple modular IBDC in Fig. 2, the transmission power P in each DAB module can be controlled by adjusting phase-shift angle D [10]:

$$P_i = \frac{n_T u_{ini} u_{oi}}{2 f_s L_T} D_i (1 - D_i) \tag{1}$$

From (1), the currents on the primary and secondary sides i_{Pi} and i_{Si} for DAB an be described as:

$$i_{ini} = \frac{n_T u_{oi}}{2 f_s L_T} D_i (1 - D_i) \ , \quad i_{oi} = \frac{n_T u_{ini}}{2 f_s L_T} D_i (1 - D_i) \tag{2}$$

Then, from topology of ISOP structure IBDC, the following equations can be obtained according to Kirchhoff's laws:

$$\begin{cases} C_{ini} \dfrac{\mathrm{d}u_{ini}}{\mathrm{d}t} = i_{in} - \dfrac{nU_o}{2 f_s L_T} D_i (1 - D_i) \\ C_o \dfrac{\mathrm{d}u_o}{\mathrm{d}t} = \displaystyle\sum_{i=1}^{n} U_{ini} \frac{nD_i(1 - D_i)}{2 f_s L_T} - \frac{u_o}{R_L} + i_o \end{cases} \tag{3}$$

Generally, to realize the IVS of DAB modules and power conversion and transmission of ISOP structure IBDC, the control structure is usually composed of IVS control loop and output voltage control loop. Therefore, the phase-shift angle D_i for each DAB module includes D_{oi} generated by output voltage control loop and D_{si} generated by IVS control loop:

$$D_i = D_{oi} - D_{si} \tag{4}$$

To obtain the small-signal model of ISOP structure IBDC, the corresponding small disturbance variables of U_{in}, U_o, u_{ini}, u_{oi}, i_{ini} , i_{oi}, D_i , D_{oi} and D_{si} are substituted into (2), and the following equation can be obtained:

$$\begin{cases} C_{in} \dfrac{\mathrm{d}\hat{u}_{ini}}{\mathrm{d}t} = \dfrac{C_{in}}{n_T} \dfrac{\mathrm{d}\hat{u}_{ini}}{\mathrm{d}t} - \dfrac{n_T u_{oi}(1 - 2D_i)}{2 f_s L_T} \widehat{D_{si}} + \dfrac{n_T u_{oi}(1 - 2D_i)}{2 f_s L_T} \displaystyle\sum_{i=1}^{n} \widehat{D}_{si} \\ C_o \dfrac{\mathrm{d}\hat{u}_{oi}}{\mathrm{d}t} = \dfrac{n_T u_{ini}(1 - 2D_i)}{2 f_s L_T} D_{oi} - \dfrac{n_T u_{oi}(1 - 2D_i)}{2 f_s L_T} \displaystyle\sum_{i=1}^{n} \widehat{D}_{si} \\ \qquad + \dfrac{n_T D_i (1 - D_i)}{2 f_s L_T} \hat{u}_{ini} - \dfrac{u_{oi}}{R_L} + i_o \end{cases} \tag{5}$$

III. The Proposed IVS Control Structure for ISOP Structure IBDC

A. Full-order model derivation under proposed IVS strategy

Based on the mathematical model, a triple-close-loop IVS control strategy is proposed for the ISOP structure IBDC, as shown in Fig. 3. From the figure, the proposed IVS scheme consists of a common output voltage control loop, the n-1 IVS control loops and n output current control loops for ISOP structure IBDC. The G_{vsi} are IVS regulators, G_{ii} are output current regulators, and G_{voi} are output voltage regulators. The common output voltage control loop is to maintain the output voltage and provide the signal to generate duty cycle for DAB

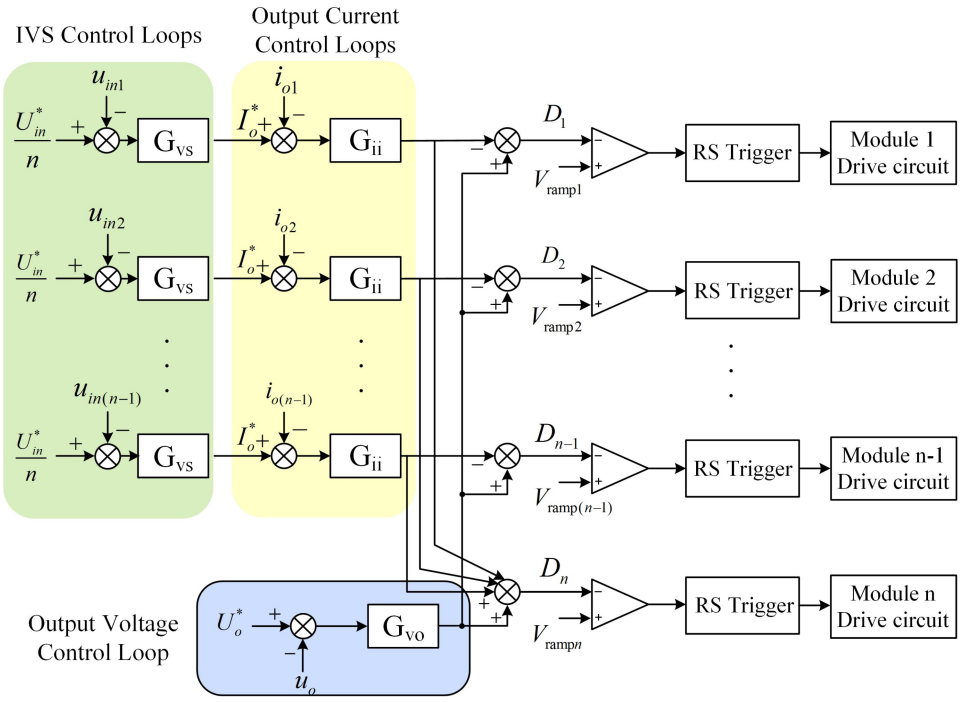

Fig. 3. The proposed triple-close-loop IVS control strategy for ISOP structure IBDC.

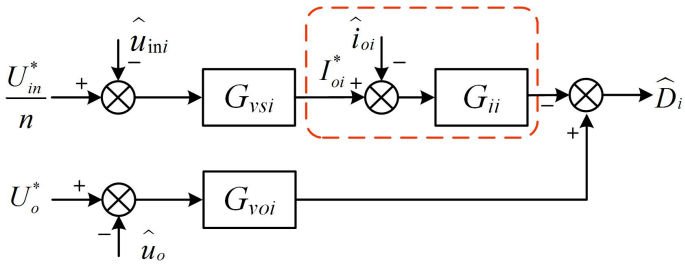

Fig. 4. The control block diagram for an individual DAB module.

modules. Since the DAB modules are connected in series on input voltage sides, the n-1 IVS control loops are set for individual DAB modules and their reference values are 1/n of input voltage U_{in}. The output signals of IVS regulators are the reference values for output current control loops. The duty cycle signals D_i for each DAB module are generated by the difference between output signals from common output voltage control loop and output current control loops. The $V_{\mathrm{RAMP}i}$ are saw-tooth wave signals, and the PWM modulation waves are obtained by comparing duty cycle signal D_i and $V_{\mathrm{RAMP}i}$.

Compared with the conventional dual-close-loop IVS control strategies, the proposed triple-close-loop IVS control strategy adds output current control loops aiming to regulate the output current and reshape the input and output impedance for DAB modules, improving the dynamic response of IVS and output steady-state characteristics of ISOP structure IBDC. When the input-voltage of individual DAB module increases, the amount of reference value of output current control loop increases, then the output of DAB module current control loop also increases, thus reducing the duty cycle and also the transmission power for DAB module. Then, the output current is reduced and the input voltage of DAB module is adjusted, maintaining the IVS for ISOP structure IBDC under the input-voltage fluctuation.

Besides, for the first n - 1 modules, the duty cycle signal are derived from output of corresponding output current control loops, and the duty cycle signal for nth module is derived from the sum of outputs of above n - 1 output current loops.

Therefore, under proposed control structure, the following equation can be obtained:

$$\sum_{i=1}^{n} \hat{D}_{si} = 0 \tag{6}$$

where D_{si} is the small-signal disturbance amount of phase-shift angle in each DAB module. Thus, the Eq. (5) can be decoupled, and the transfer function matrix of ISOP structure IBDC is:

$$\begin{bmatrix} \hat{u}_{\mathrm{in}1} \\ \hat{u}_{\mathrm{in}2} \\ \vdots \\ \hat{u}_{\mathrm{in}n} \\ \hat{u}_{\mathrm{o}} \end{bmatrix} = \begin{bmatrix} A(s) & 0 & \cdots & 0 & 0 \\ 0 & A(s) & \cdots & 0 & 0 \\ \vdots & \vdots & \cdots & \vdots & \vdots \\ 0 & 0 & \cdots & A(s) & 0 \\ 0 & 0 & \cdots & 0 & B(s) \end{bmatrix} = \begin{bmatrix} \hat{D}_{s1} \\ \hat{D}_{s2} \\ \vdots \\ \hat{D}_{sn} \\ \hat{D} \end{bmatrix} \tag{7}$$

where

$$\begin{cases} A(s) = G_{u_{\mathrm{in}i}D_{si}} = \left.\dfrac{\hat{u}_{\mathrm{in}i}}{\hat{D}_{si}}\right|_{\substack{\hat{D}=0 \\ \hat{D}_{sj}=0(i\neq j)}} = \dfrac{nU_{\mathrm{o}}(1-2D)}{sC_1 2f_{\mathrm{s}}L_{\mathrm{T}}} \\ B(s) = G_{u_{\mathrm{o}}D} = \left.\dfrac{\hat{u}_{\mathrm{o}}}{\hat{D}}\right|_{\substack{\hat{u}_{\mathrm{in}}=0 \\ \hat{D}_{si}=0}} = \dfrac{nU_{\mathrm{in}}(1-2D)}{2f_s L_T(sC_2+1/R_{\mathrm{L}})} \end{cases} \tag{8}$$

From (6) ~ (8), the control of each DAB module in ISOP structure IBDC can be decoupled from each other, realizing the small signal input impedance decoupling of each single-input single-output modules. Then, input impedance of each DAB module can be analyzed and designed independently.

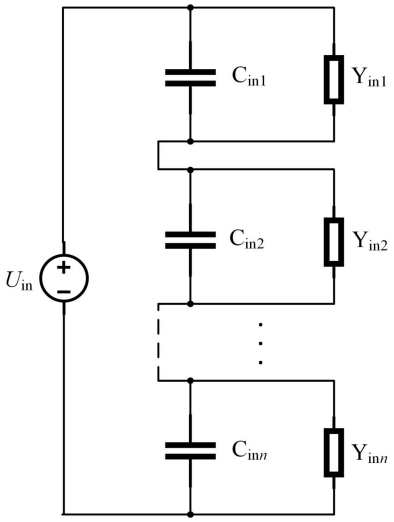

Fig. 5. The equivalent input impedance for ISOP structure IBDC.

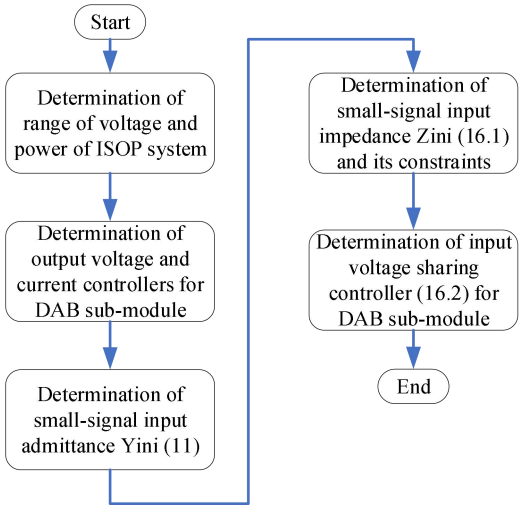

Fig. 6. The design process of proposed IVS strategy.

Since the IVS control loop and output voltage control loop in ISOP structure IBDC system are decoupled, the control block diagram for a single DAB module under proposed IVS strategy are presented in Fig. 4. According to the figure, the small signal expression of phase-shift angle can be described as:

$$\widehat{D}_i = G_{voi}\hat{u}_o - \left(G_{vsi}\hat{u}_{ini} - \hat{i}_{oi}\right)\cdot G_{ii} \tag{9}$$

Therefore, the small-signal model of DAB module under the proposed IVS control strategy can be described as:

$$\begin{cases} \tilde{i}_{ini} = G_{i_{ini}d}\cdot\left(\left(G_{voi}\hat{u}_o + \hat{i}_{ini}\right)\cdot G_{ii} - G_{vsi}\hat{u}_{ini}\right) + G_{i_{ini}u_o}\cdot\tilde{u}_o \\ \tilde{i}_{oi} = G_{i_{oi}d}\cdot\left(\left(G_{voi}\hat{u}_o + \hat{i}_{oi}\right)\cdot G_{ii} - G_{vsi}\hat{u}_{ini}\right) + G_{i_{oi}u_{in}}\cdot\tilde{u}_{ini} \\ \tilde{u}_{oi} = \tilde{i}_{oi}\cdot Z_{load} \\ Z_{load} = R_L/\left(1+sR_LC_2\right) \end{cases} \tag{10}$$

where Z_{load} is the load impedance. From (10), the corresponding small-signal input admittance Y_{ini} of DAB module is:

$$Y_{ini} = G_{i_{ini}d}\cdot G_{vsi}\cdot G_{ii} + \frac{\left(G_{i_{oi}d}\cdot G_{vsi}\cdot G_{ii} + G_{i_{oi}u_{in}}\right)\cdot\left[\left(G_{i_{ini}u_o} - G_{i_{ini}d}\cdot G_{voi}\right)\cdot Z_{load} + G_{i_{oi}d}\cdot G_{ii}\right]}{1 + G_{i_{oi}d}\cdot G_{voi}\cdot Z_{load} - G_{i_{oi}d}\cdot G_{ii}} \tag{11}$$

Under conventional IVS strategy, the design of IVS loop is based on input impedance $-V^2/P$, which ignores high-order components and the influence between input and output control loop. From (11), under the proposed IVS strategy, the small-signal input impedance model contains dynamic characteristics of all controllers and high-order components, thus a full-order model for DAB module is established, making DAB module and ISOP structure IBDC obtain the larger bandwidth, higher low-frequency gain and better dynamic response and stability characteristic when disturbance and fluctuation occur.

B. Design process of proposed IVS strategy

From (11) and considering the input capacitance, the closed-loop input impedance of a single DAB module is:

$$Z_{ini} = \frac{1}{sC_i + Y_{ini}} \tag{12}$$

Besides, the DAB modules are connected in series on the input side, thus the total input impedance of ISOP structure IBDC can be expressed as:

$$Z_{in} = \sum_{i=1}^{n} Z_{ini} \tag{13}$$

From (10) ~ (13), the equivalent input impedance for ISOP structure IBDC is presented in Fig. 5. According to the figure, the equivalent input admittance Y_{ini} is connected paralleled to the input capacitance C_{ini}. Considering input voltage difference between two adjacent DAB modules:

$$\begin{aligned} \Delta V_{ab} &= V_{ina} - V_{inb} = \frac{Z_{ina} - Z_{inb}}{Z_{in}} \\ &= \frac{Y_{ina} - Y_{inb}}{\sum_{i=1}^{n}\left(\prod_{j\neq i}^{n}\left(sC_{inj} + Y_{inj}\right)\right)Z_{in}}\prod_{i\neq a,b}^{n}\left(sC_{ini} + Y_{ini}\right) \end{aligned} \tag{14}$$

During practical applications, the input capacitors are not usually equaled, thus $C_{in1} \neq C_{in2} \neq \ldots \neq C_{ini} \neq C$. However, for the input admittance Y_{ini}, when the order of numerator becomes greater than the order of denominator, from (13), the following equation can be realized:

$$\lim_{t\to\infty}\Delta V_{ab}(t) = \lim_{s\to 0}\Delta V_{ab}(s) = 0 \tag{15}$$

According to (15), the IVS control for ISOP system can be achieved. Since a single DAB module can realize independent control according to aforementioned analysis, input impedance bandwidth needs to reach 1/15 ~ 1/20 of switching frequency to maintain ideal dynamic and steady-state characteristics, and maintaining a low-order system is beneficial to the adjustment of system. Therefore, from the closed-loop input impedance of a single DAB module and to guarantee the bandwidth is 1/15 ~ 1/20 of switching frequency and damping ratio in a second-order system is 0.707, the input impedance of a DAB module under proposed IVS strategy can be described as:

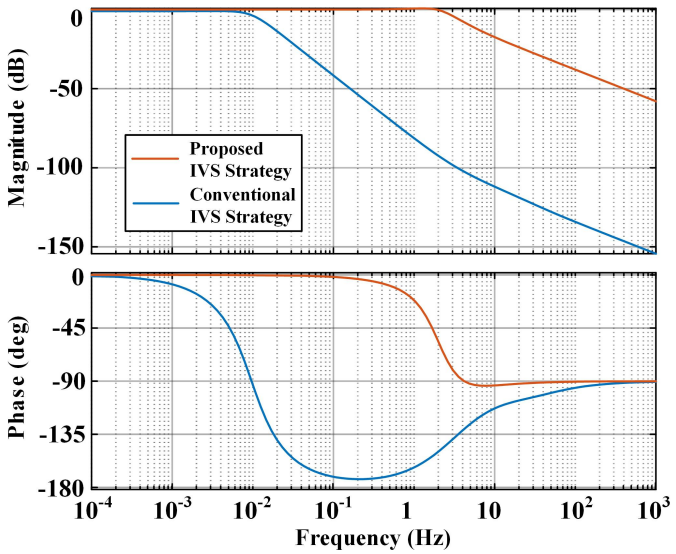

Fig. 7. Comparison of system performance of input impedance under conventional and proposed IVS strategy.

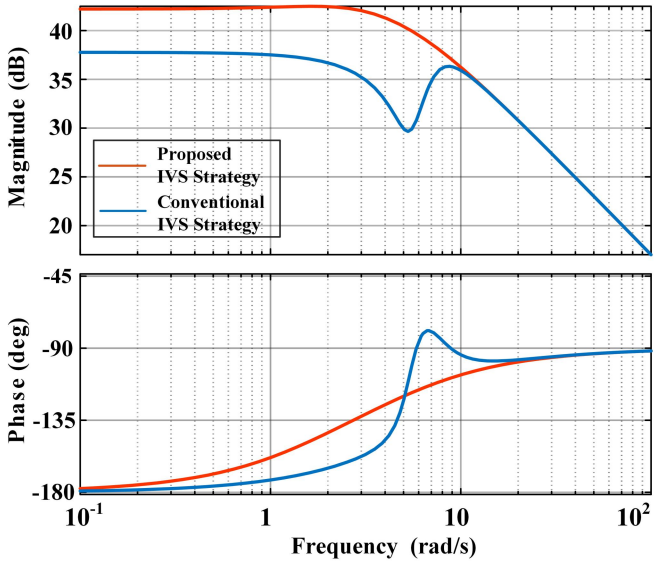

Fig. 8. Comparison of system performance of output impedance under conventional and proposed IVS strategy.

$$\begin{cases} Z_{ini} = \dfrac{1}{sC + Y_{ini}} \\ G_{vsi} = \dfrac{Y_{eq} - G_{i_{1i}d} G_{vsi}}{G_{i_{2i}d} T_{vi}} = \dfrac{Y_i - G_{i_{1i}d} G_{vsi}}{G_{i_{2i}d} T_{vi}} \end{cases} \tag{16}$$

The input admittance Y_{ini} is designed to equaled to equivalent admittance Y_{eq}:

$$Y_{eq} = \begin{cases} R_{eq} \\ R_{eq} + sC_{eq} \quad \Rightarrow \xi = 0.707 \\ R_{eq} + 1/sL_{eq} \end{cases} \tag{17}$$

From (11) and (17), the input voltage sharing controller under proposed IVS strategy can be designed as:

$$G_{vsi} = \frac{Y_{eq} - T_{Y_{ini}}}{G_{i_{oi}d} G_{ii}} \tag{18}$$

where

$$T_{Y_{ini}} = \frac{\left(G_{i_{oi}d} \cdot G_{vsi} \cdot G_{ii} + G_{i_{oi}u_{in}}\right) \cdot \left[\left(G_{i_{ini}u_o} - G_{i_{ini}d} \cdot G_{voi}\right) \cdot Z_{load} + G_{i_{oi}d} \cdot G_{ii}\right]}{1 + G_{i_{oi}d} \cdot G_{voi} \cdot Z_{load} - G_{i_{oi}d} \cdot G_{ii}}$$

According to the analysis above, the design process for the proposed IVS strategy is presented in Fig. 6. From the figure, the circuit parameters, voltage level and power rantings of ISOP structure IBDC is determined, and then the output voltage controller and output current controllers for individual DAB module are designed accordingly. Based on small-signal input impedance model of DAB module Y_{ini} in (11), the total input impedance model of ISOP structure IBDC Zin can be achieved, and then the corresponding IVS controllers for DAB modules can be obtained.

IV. System Characteristics Analysis for Proposed IVS Control Strategy

A. Input impedance analysis under proposed control strategy

According to (16), the frequency response characteristics and comparison of system performance of input impedance under conventional and proposed IVS strategy are presented in Fig. 7. According to the figure, both of the conventional and proposed IVS strategies have no poles and zeros in the right half plane in the phase frequency response, ensuring the stable operation of ISOP structure IBDC system. Besides, due to the full-order small-signal input impedance in established for DAB modules under proposed IVS strategy, a wider bandwidth is achieved and a higher gain is also obtained for ISOP structure IBDC.

Moreover, the larger gain margin and phase margin are realized under the proposed IVS strategy, thus the shorter dynamic response and adjusting time, smaller overshoot and output voltage ripple can be obtained for ISOP structure IBDC under the fluctuation or disturbance in the input voltage during practical operation.

B. Output impedance analysis under proposed control strategy

In addition to input impedance, the output impedance is also studied for ISOP structure IBDC. From (9) and (10), the output impedance Z_{oi} of a DAB module under proposed IVS strategy can be obtained as:

$$Z_{oi} = \frac{1 - G_{i_{oi}d} \cdot G_{ii} + \dfrac{G_{i_{ini}d} \cdot G_{ii} \cdot \left(G_{i_{oi}d} \cdot G_{vsi} \cdot G_{ii} + G_{i_{oi}u_{in}}\right)}{G_{i_{ini}d} \cdot G_{vsi} \cdot G_{ii}}}{-G_{i_{oi}d} \cdot G_{voi} - \dfrac{\left(G_{i_{ini}u_o} - G_{i_{ini}d} \cdot G_{voi}\right) \cdot \left(G_{i_{oi}d} \cdot G_{vsi} \cdot G_{ii} + G_{i_{oi}u_{in}}\right)}{G_{i_{oi}d} \cdot G_{vsi} \cdot G_{ii}}} \tag{19}$$

According to (19), the frequency response characteristics and comparison of system performance of output impedance under conventional and proposed IVS strategy are presented in Fig. 8. According to the figure, compared to conventional IVS

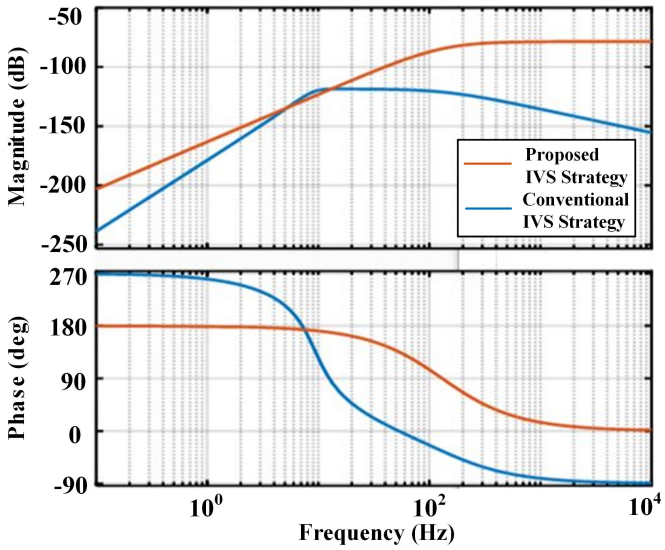

Fig. 9. The Bode diagram of audio susceptibility of IBDC under the conventional and proposed IVS strategy.

TABLE I
The Parameters of IBDC and Experiment Setup

Symbol	Electrical Parameters	Quantity
U_{in}	Input DC Voltage	100 ~ 200 V
U_o	Output DC Voltage	20 ~ 80 V
P	Rated Power of IBDC	1kW
n	Number of DAB Modules	2
f_s	Switching Frequency	22k Hz
C_1 , C_2	Capacitance in DAB Module	141 μF
n_T	HFL Transformer Voltage Ratio	3 : 2
L_T	HFL Equivalent Inductance	30 μH

strategy, the proposed strategy receives higher gain and wider bandwidth in low-frequency range, thus the ISOP structure IBDC can achieve faster dynamic response, smaller overshoot, better resonance suppression and more stable output steady-state characteristics under the fluctuation or disturbance in connected load. In addition, the output impedance frequency characteristics under proposed strategy are almost the same with that under conventional strategy in high-frequency range. That's because the output voltage of ISOP structure IBDC is filtered by output capacitance, thus effectively suppressing the high-frequency ripple.

C. Audio-susceptibility under proposed control strategy

According to [37], the audio susceptibility of converter can be defined as:

$$A_s = \frac{G_{\text{uinuo}}}{1 + T_{\text{loop}}} \tag{20}$$

where T_{loop} is the gain of control loop, and G_{uinuo} is the input-to-output transfer function.

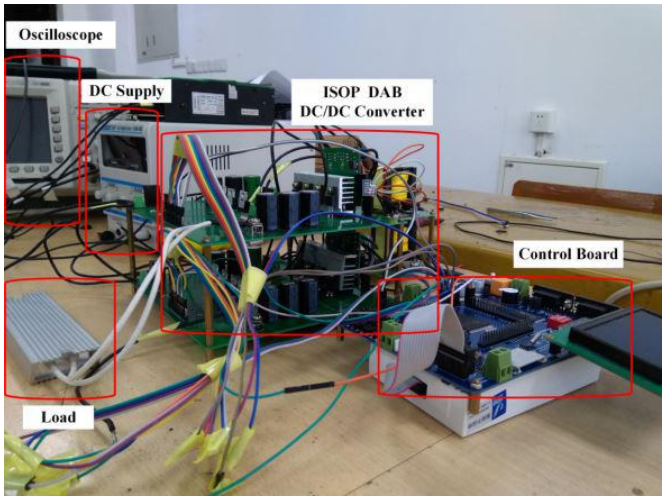

Fig. 10. The prototype and experiment setup of ISOP structure IBDC

According to (20) and for the ISOP structure IBDC under proposed IVS strategy, the T_{loop} equals to $G_{\text{vs1}} \times G_{\text{ii}} \times G_{\text{uind}}$, where G_{vuind} is the, G_{ii} is output current regulators, and G_{vs1} is the IVS controller designed according to (18). Besides, T_{loop} of IBDC under conventional IVS strategy equals to $G_{\text{vs2}} \times G_{\text{uind}}$, where G_{vs2} is the IVS controller designed with a PI controller [38]. Moreover, the audio susceptibility for ISOP structure IBDC under the conventional and proposed IVS strategies are depicted in Fig. 9. As can be seen from the figure, compared with the conventional IVS strategy, the proposed IVS strategy provides an extra attenuation in low-frequency band and high-frequency band compared with that under conventional IVS strategy. Although the gain of proposed IVS strategy is finite, it is still relatively high for reducing the steady-state error.

V. Experimental Verification

To verify the analysis and proposed control strategy, a ISOP structure IBDC prototype based on DAB module is established in the laboratory, as shown in Fig. 10, and the parameters and experiment setup is presented in Table I.

Based on parameters in Table I, the IVS and output voltage controller under conventional IVS strategy are G_{ui} = 50+600/s and G_{uo} = 15+200/s, and the IVS, output current and voltage controller under proposed IVS strategy are G_{vs} = 50+600/s+7s, G_{i} =15+3000/s and G_{uo} = 15+200/s, respectively. When input DC voltage is U_{in} = 150V and the preset output DC voltage is U_o = 45V, the steady-state experiment results of ISOP structure IBDC under proposed IVS control strategy are shown in Fig. 11. From Fig. 11(a), the input voltages for each DAB module are both maintained at $U_{\text{in1}} = U_{\text{in2}} = U_{\text{in}} / 2 = 75$V, realizing the ideal IVS performance. Besides, the output voltage of IBDC are controlled at preset value U_o = 45V, and no oscillation occurs in DC voltage. In addition, the HFL voltages and current in an individual DAB module are shown in Fig. 11(b), realizing voltage conversion and power transmission for DAB module and ISOP structure IBDC. The steady-state experiment results reflect that, under the proposed IVS control strategy, the ideal IVS is realized for DAB modules, and the ISOP structure IBDC also operates normally and stably, realizing voltage conversion and power transmission for DC distribution network.

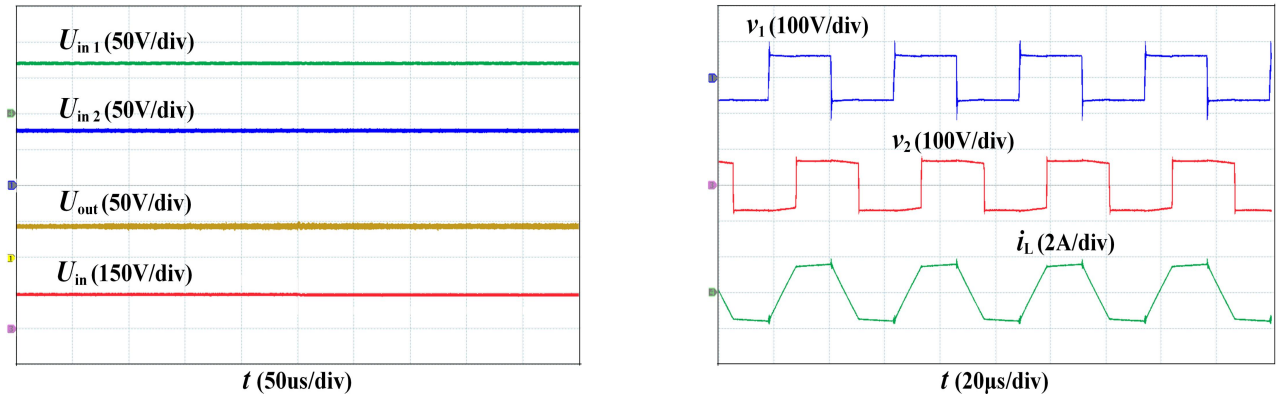

(a) (b)

Fig. 11. Steady-state experiment results of ISOP structure IBDC under proposed control strategy. (a) Input and output voltages in a IBDC, (b) HFL voltages and current in a DAB module.

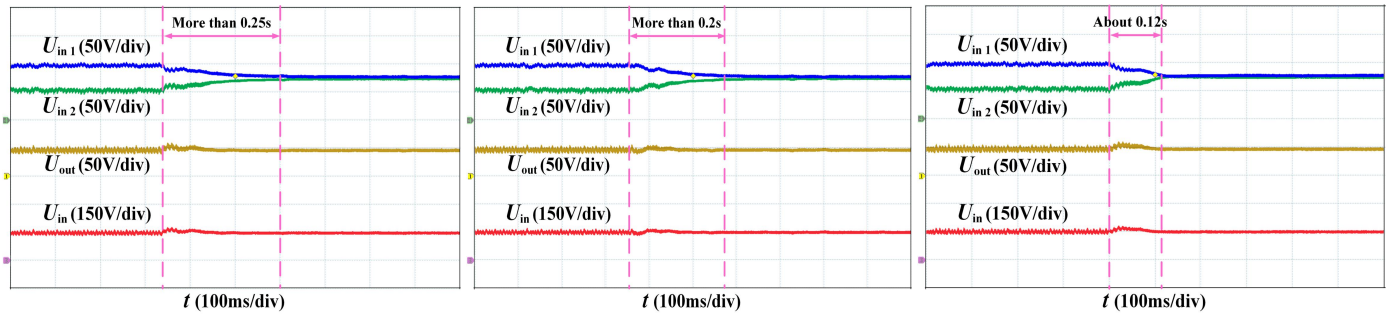

(a) (b) (c)

Fig. 12. Input and output voltages of IBDC when IVS strategy starts working. (a) Conventional IVS strategy, (b) CFOCS without IVS loops, (c) Proposed IVS strategy.

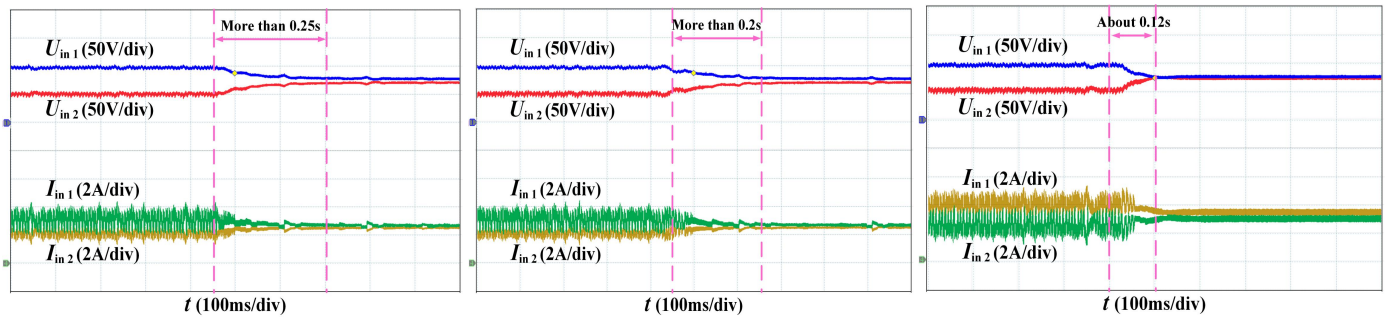

(a) (b) (c)

Fig. 13. Voltages and currents of DAB module when IVS strategy starts working. (a) Conventional IVS strategy, (b) CFOCS without IVS loops, (c) Proposed IVS strategy.

When the IVS strategy is put into operation during start-up period, the voltages and currents of ISOP structure IBDC and DAB modules under the conventional IVS strategy, the cross feedback output current sharing (CFOCS) strategy without IVS loops and proposed IVS strategy are compared and presented in Fig. 12 and Fig.13, respectively. From Fig. 12(a), Fig. 12(b), Fig. 13(a) and Fig. 13(b), the adjusting time of input voltages in IBDC and DAB modules is about 0.25s and 0.2s under conventional IVS strategy with constant input impedance and the CFOCS strategy without IVS loops, respectively, and the input voltages in DAB modules are not fully balanced. Besides, there are low-frequency oscillations in the input voltage and current of each DAB module, and this is not conducive to the long-term stable operation of DAB module. Correspondingly, the adjusting time of input voltages in DAB modules is about 0.12s with a smooth switching process under proposed strategy, as shown in Fig. 12(c) and and Fig. 13(c). Besides, the input voltages in DAB modules are practically balanced, and there are no low-frequency oscillations in the input voltages and currents of each DAB module. Therefore, the experiment results reflect that, compared with conventional IVS control strategy, the proposed IVS control strategy obtains the shorter adjusting time and smoother realization process during start-up period, and also achieves better IVS performance with ideal voltage and current characteristics in DAB module and ISOP structure IBDC.

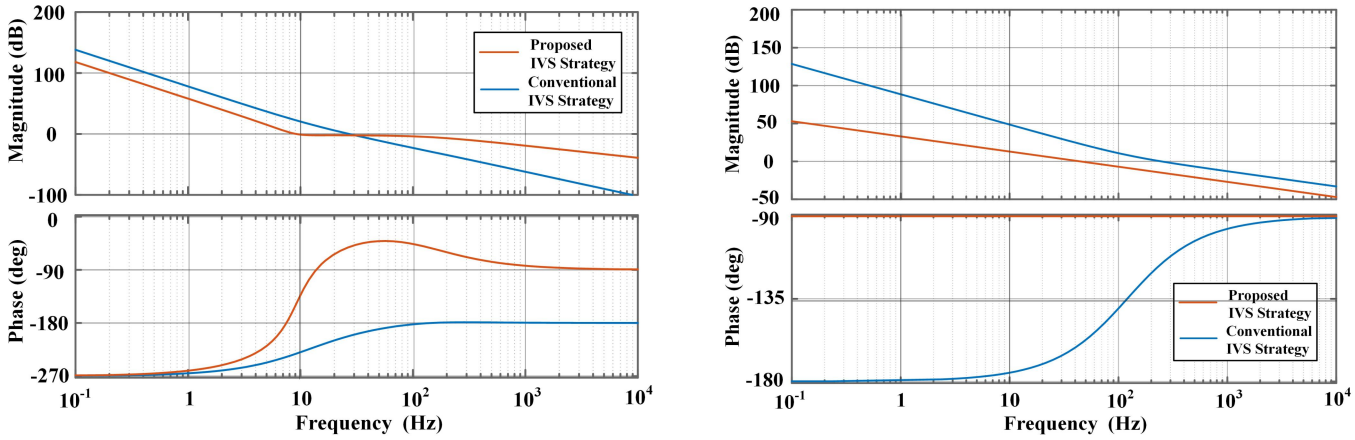

Fig. 14. The current and voltage loop-gains for experimental case. (a) Voltage loop gain, (b) Current loop gain.

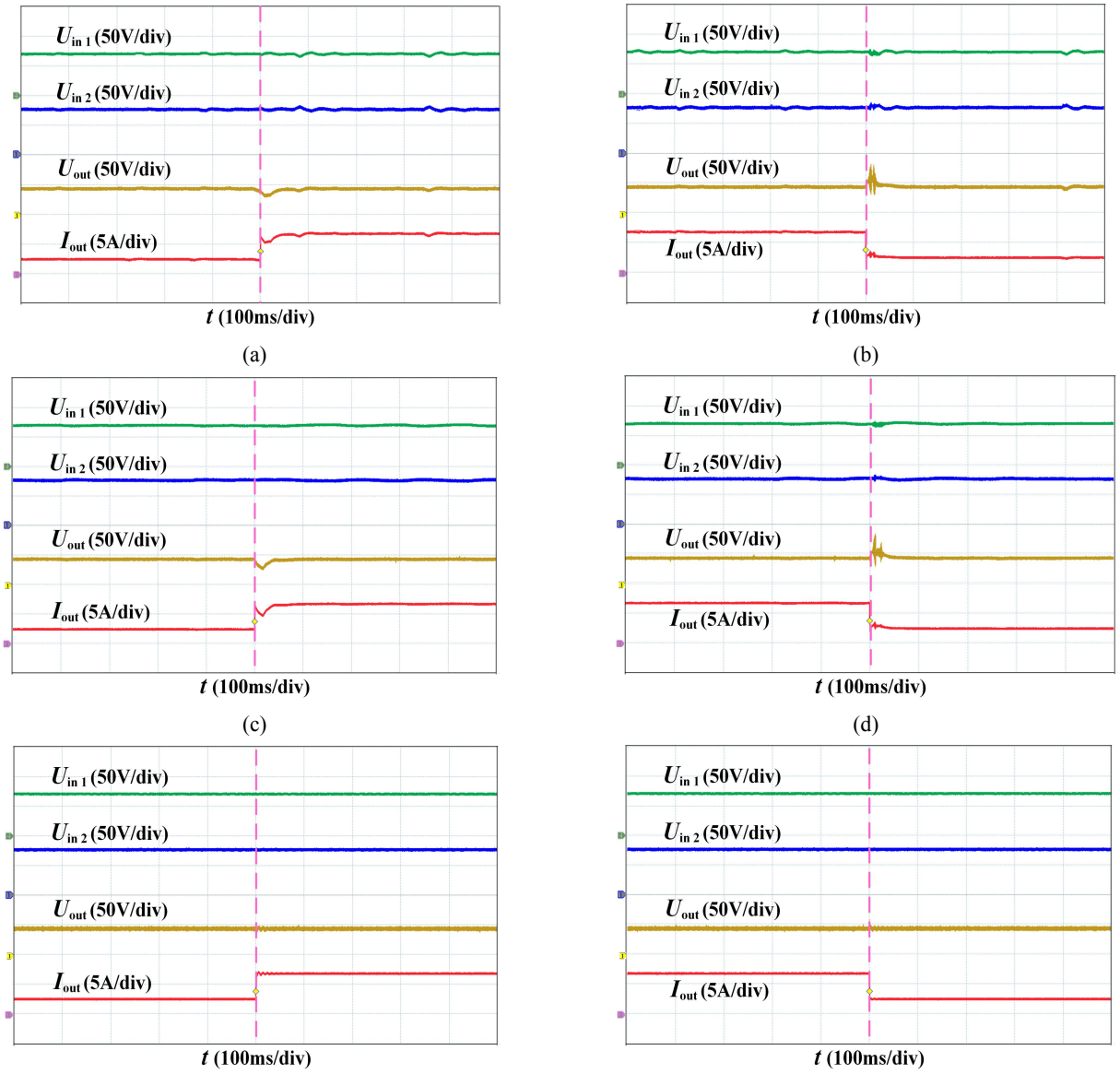

Fig. 15. Output voltages and currents of ISOP structure IBDC when the connecting load varies suddenly. (a) Conventional IVS strategy under load decrease, (b) Conventional IVS strategy under load increase, (c) CFOCS without IVS loops under load decrease, (d) CFOCS without IVS loops under load increase, (e) Proposed IVS strategy under load decrease, (f) Proposed IVS strategy under load increase.

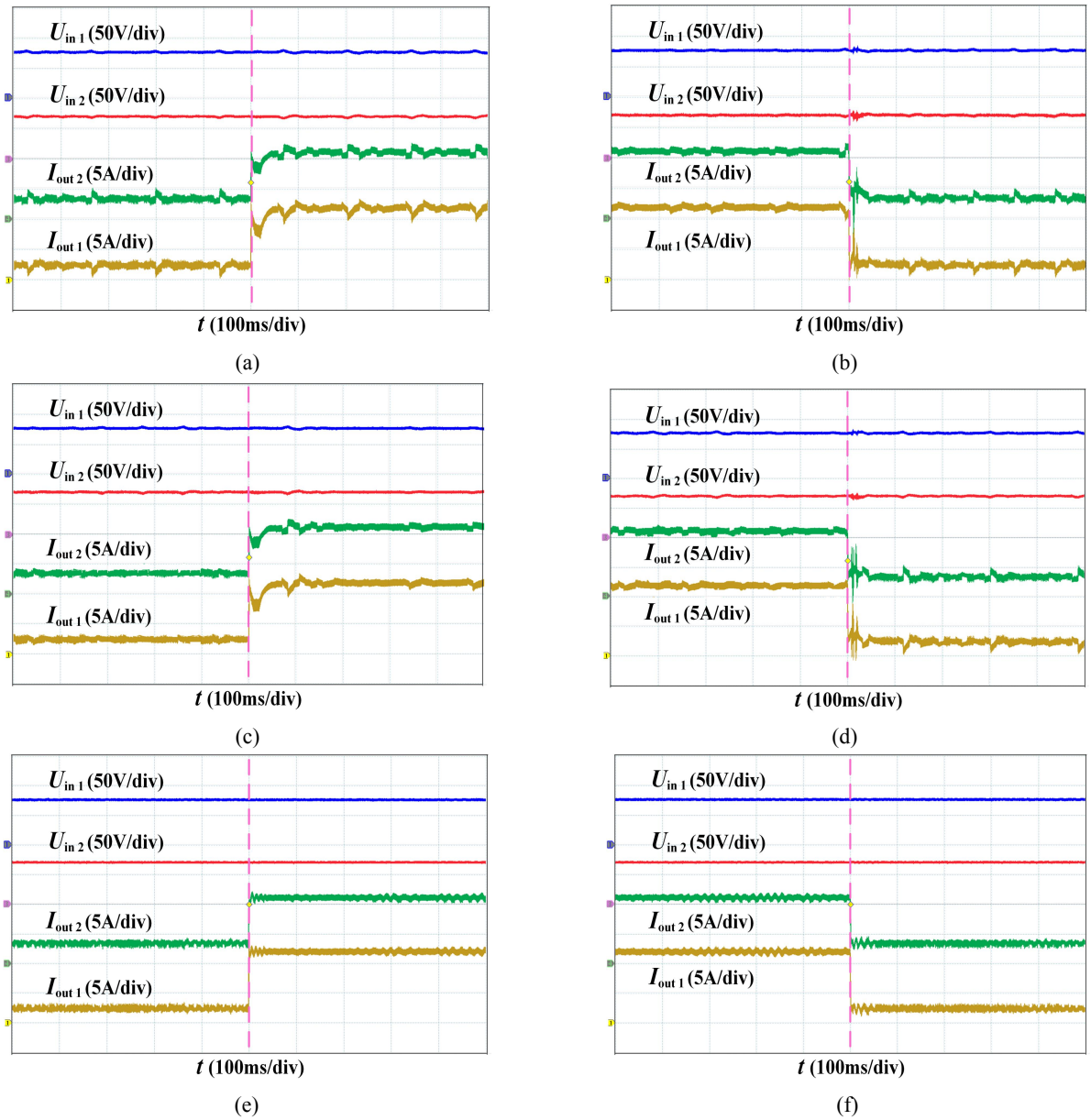

Fig. 16. Output voltages and currents of DAB module when the connecting load varies suddenly. (a) Conventional IVS strategy under load decrease, (b) Conventional IVS strategy under load increase, (c) CFOCS without IVS loops under load decrease, (d) CFOCS without IVS loops under load increase, (e) Proposed IVS strategy under load decrease, (f) Proposed IVS strategy under load increase.

Besides, based on the parameters in Table I and the control parameters design for IBDC, the Bode diagrams of voltage and current loop of IBDC under conventional and proposed IVS strategy are presented in Fig. 14. According to the voltage loop shown in Fig. 14(a), the phase margin and gain margin under conventional IVS strategy are PM = -21.9 and GM = 29dB, respectively, and phase margin and gain margin under proposed IVS strategy are PM = 32.3, GM = 4.11dB, respectively. In addition, according to the current loop shown in Fig. 14(b), no output current control loop under conventional IVS strategy, and phase margin under proposed IVS strategy are PM = 62.4. From the analysis above, the IBDC obtains better voltage and current control characteristics under proposed IVS strategy.

When the connecting load varies suddenly, the input and output voltages and currents of ISOP structure IBDC and DAB modules under the conventional IVS strategy, CFOCS strategy without IVS loops and proposed IVS strategies are compared and presented in Fig. 15 and Fig.16, respectively. According to Fig. 15(a) and Fig. 15(c), when the connecting load decreases, the dynamic response and adjusting time of input and output voltages and currents in ISOP structure IBDC is about 0.15s and 0.1s under conventional IVS strategy with constant input impedance and the CFOCS without IVS loops, respectively, and the overshoots and oscillation occur in input and output voltages and currents. That may cause false protection and potential instability in high-voltage and large-current scenario. Besides, the slow dynamic response, large overshoots and oscillation also occur in voltage and current of individual DAB module, as shown in Fig. 16(a) and Fig. 16(c), leading to a low power quality and adversely affecting the stable operation of DAB module, and it is prone to problems such as heat loss, over-voltage and over-current breakdowns. Correspondingly,

under the proposed IVS strategy, when the connecting load decreases suddenly, the dynamic response and adjusting time of input and output voltages and currents in both IBDC and DAB modules are less than 0.02s with a smooth switching process, as shown in Fig. 15(e) and Fig. 16(e). Besides, no low-frequency oscillations emerge in the output voltage and current in DAB modules, and the voltage and current ripples are also small.

Moreover, the similar experimental results occur when the connecting load increases, as shown in Fig. 15(b), Fig.15(d), Fig.15(f), Fig. 16(b), Fig. 16(d) and Fig.16(f). The experiment results reflect that, compared with conventional IVS strategy and CFOCS strategy without IVS loops, the proposed IVS strategy eliminates influences from connected load fluctuation to IVS performance, realizing ideal dynamic characteristics and avoiding the false protection actuation and potential instability caused by overshoots and oscillation in high voltage and large current scenario. Besides, the proposed IVS strategy maintains the high output power quality and stable operation for DAB module and ISOP structure IBDC during connecting load variation, thus increasing the adaptability and practicability for ISOP structure IBDC, especially suitable for the application in DC distribution networks with distributed sources, variable operating voltages and diverse loads.

Moreover, to further verify the performance of IBDC under proposed strategy, the experimental comparisons of adjusting time and overshoot under conventional and proposed strategy with different variation range of input-voltage and connected-load are shown in Fig. 17. As can be seen from Fig. 17(a) and Fig. 17(b), with different variation range of input-voltage and connected-load, the adjusting time of input-voltage and output voltage and current during dynamic process under proposed strategy are smaller than that under the conventional strategy. Besides, with different variation range of input-voltage and connected-load, the overshot of voltage and current during dynamic process under proposed strategy are also smaller than that under the conventional strategy, as shown in Fig. 17(c) and Fig. 17(d), avoiding false protection and potential instability for ISOP structure IBDC. The experimental results further verifies that the ISOP structure IBDC scheme obtains better dynamics response characteristics and maintain ideal output power and stable operation under proposed IVS control strategy.

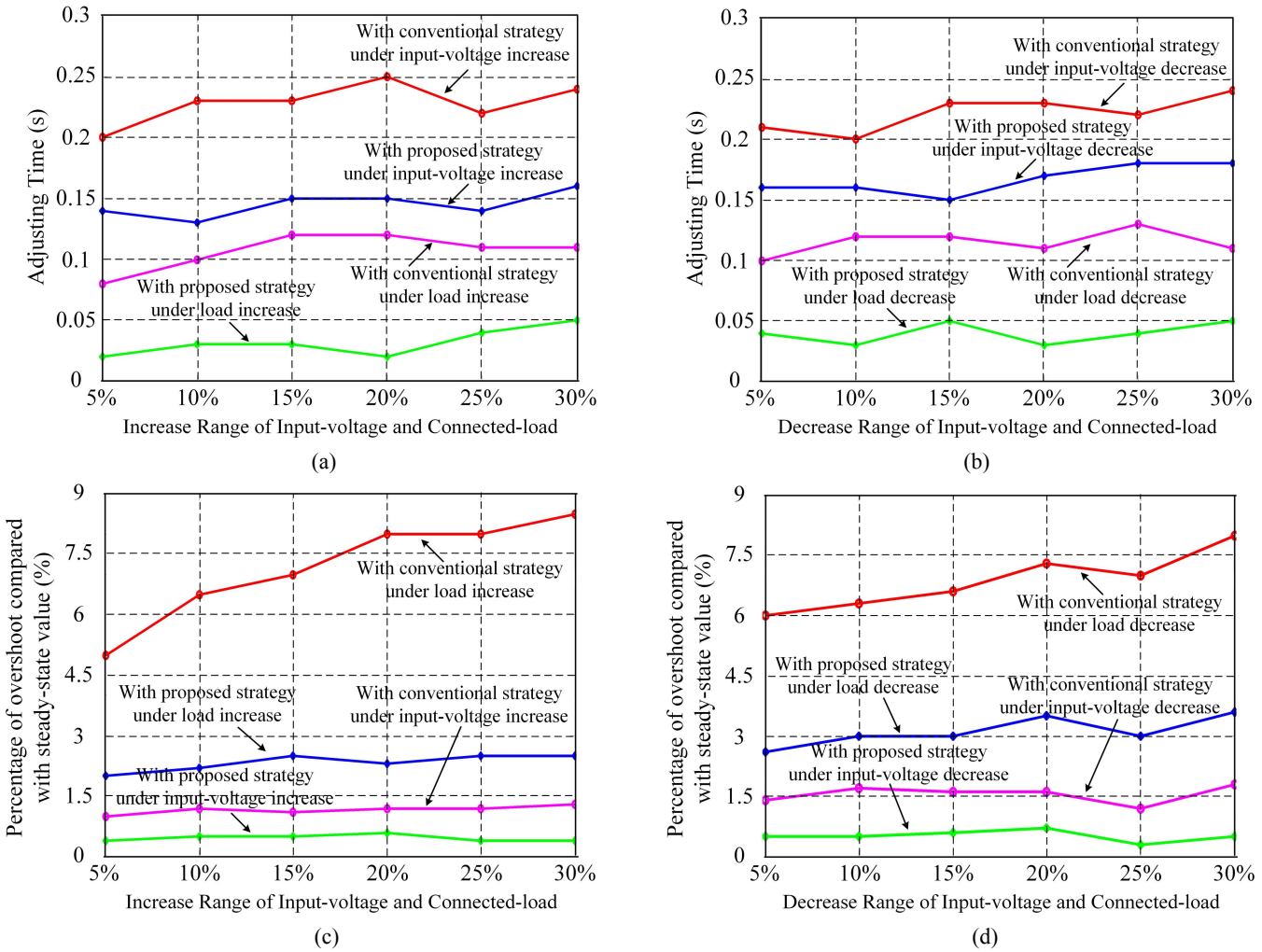

Fig. 17. Comparisons of adjusting time and overshoot under conventional and proposed IVS strategy. (a) Adjusting time with different increase range of input-voltage and load, (b) Adjusting time with different decrease range of input-voltage and load, (c) Overshoot with different increase range of input-voltage and load, (d) Overshoot with different decrease range of input-voltage and load.

VI. Conclusion

To improve the dynamic and steady-state performance for ISOP structure IBDC under frequent and greater fluctuations in bus voltage and connected load in DC distribution networks, this paper proposes a triple-close-loop IVS control strategy for ISOP structure IBDC. By adding output current control loops based on conventional IVS strategy, the proposed IVS strategy reshapes small-signal input and output impedance. Compared with the conventional strategy with constant input impedance, the reshaped input impedance is a full-order model containing high-order components and sensitive to output voltage, and the designed IVS control based on reshaped input impedance can improve the dynamics characteristics, maintain ideal output power and avoid false protection and potential instability for ISOP structure IBDC under the frequent and large fluctuation, providing a feasible, efficient and practical control scheme for ISOP structure IBDC. However, the proposed IVS strategy has drawbacks such as extra design steps and burden, complicated parameter calculation. Thus, the future works on simplified structure and improved adaptability for the proposed strategy should be considered, and the implementation on other multiple modular structures IBDC such as ISOS and IPOS system needs further investigation, promoting the engineering application of proposed strategy and the development for both the multiple modular IBDC and DC distribution networks.

References

[1] A. Francés, R. Asensi, Ó. García, R. Prieto, and J. Uceda, "Modeling electronic power converters in smart DC microgrids - an overview," *IEEE Trans. Smart Grid*, vol. 9, no. 6, pp. 6274 - 6287, Nov. 2018.

[2] F. Nejabatkhah and Y. W. Li, "Overview of power management strategies of hybrid AC/DC microgrid," *IEEE Trans. Power Electron*., vol. 30, no. 12, pp. 1038 - 1044, Dec. 2015.

[3] T. Dragicevic, X. Lu, J. C. Vasquez, and J. M. Guerrero, "DC microgrids - Part I: a review of control strategies and stabilization techniques", I*EEE Trans. Power Electron.*, vol. 31, no. 7, pp. 4876 - 4891, Jul. 2016.

[4] T. Dragicevic, X. Lu, J. C. Vasquez, and J. M. Guerrero, "DC microgrids -Part II: a review of power architectures, applications, and standardization issues", *IEEE Trans. Power Electron.*, vol. 31, no. 5, pp. 3528 - 3549, May 2016.

[5] Y. Wang, Q. Song, Q. Sun, B. Zhao, J. Li and W. Liu, "Multilevel MVDC link strategy of high-frequency-link DC transformer based on switched capacitor for MVDC power distribution," *IEEE Trans. Ind. Electron.*, vol. 64, no. 4, pp. 2829 - 2835, Apr. 2017.

[6] M. Mehrasa, E. Pouresmaeil, S. Zabihi, and J. Catalão, "Dynamic model, control and stability analysis of MMC in HVDC transmission systems," *IEEE Trans. Power Delivery*, vol. 32, no. 3, pp. 1471 - 1482, Jun. 2017.

[7] B. Zhao, Q. Song, J. Li, Q. Sun, and W. Liu, "Full-process operation, control and experiments of modular high-frequency link DC transformer based on dual-active-bridge for flexible MVDC distribution: a practical tutorial", *IEEE Trans. Power Electron*., vol. 32, no. 9, pp. 6751 - 6766, Sept. 2017.

[8] J. E. Huber and J. W. Kolar, "Applicability of solid-state transformers in today's and future distribution grids," *IEEE Trans. Smart Grid*, vol. 10, no. 1, pp. 317 - 326, Jan. 2019.

[9] J. D. Páez, D. Frey, J. Maneiro, S. Bacha, and P. Dworakowski, "Overview of DC-DC converters dedicated to HVDC grids," *IEEE Trans. Power Delivery*, vol. 34, no. 1, pp. 119 - 128, Feb. 2019.

[10] B. Zhao, Q. Song, W. Liu and Y. Sun, "Overview of dual-active-bridge isolated bidirectional dc-dc converter for high-frequency-link power-conversion system," *IEEE Trans. Power Electron.*, vol. 29, no. 8, pp. 4091 - 4106, Aug. 2014.

[11] I. A. Gowaid, G. P. Adam, S. Ahmed, D. Holliday and B. W. Williams, "Analysis and design of a modular multilevel converter with trapezoidal modulation for medium and high voltage DC-DC transformers," *IEEE Trans. Power Electron.*, vol. 30, no. 10, pp. 5439 - 5457, Oct. 2015.

[12] Y. Wang, Q. Song, B. Zhao, J. Li, Q. Sun, and W. Liu, "Quasi-square-wave modulation of modular multilevel high-frequency DC converter for medium-voltage DC distribution application," *IEEE Trans. Power Electron.*, vol. 33, no. 9, pp. 7480 - 7495, Sept. 2018.

[13] A. Mohammadpour, L. Parsa, M. H. Todorovic, R. Lai, R. Datta, and L. Garces. "Series-input parallel-output modular-phase DC-DC converter with soft-switching and high-frequency isolation", *IEEE Trans. Power Electron*., vol. 31, no. 1, pp. 111 - 119, Jan. 2016.

[14] D. Sha, Z. Guo, T. Luo, and X. Liao, "A general control strategy for input-series–output-series modular DC–DC converters", *IEEE Trans. Power Electron.*, vol. 29, no. 7, pp. 3766 - 3775, Jul. 2014.

[15] Z. Guo, D. Sha, and K. Song, "Output-series connected dual active bridge converters for zero-voltage switching throughout full load range by employing auxiliary LC networks", *IEEE Trans. Power Electron*., vol. 34, no. 6, pp. 5549 - 5562, Jun. 2019.

[16] M. Guan, "A series-connected offshore wind farm based on modular dual-active-bridge (DAB) isolated DC-DC converter", *IEEE Trans. Energy Conversion*, vol. 34, no. 3, pp. 1422 - 1431, Sept. 2019.

[17] Y. Wang, S. Z. Chen, Y. Z. Wang, L. Zhu, Y. Guan, G. Zhang, L. Yang, and Y. Zhang, "A multiple modular isolated DC/DC converter with bidirectional fault handling and efficient energy conversion for DC distribution network", *IEEE Trans. Power Electron*., vol. 35, no. 11, pp. 11502 - 11517, Nov. 2020.

[18] P. Zumel, L. Ortega, A. Lázaro,C. Fernández, A. Barrado, A. Rodríguez, , and M. Hernando, "Modular dual-active bridge converter architecture", *IEEE Trans. Ind. Appl.*, vol. 52, no. 3, pp. 2444 - 2455, May 2016.

[19] W. Chen , X. Fu, C. Xue , H. Ye, W. A. Syed, L. Shu ,G. Ning, and X. Wu, "Indirect input-series output-parallel DC–DC full bridge converter system based on asymmetric pulsewidth modulation control strategy", *IEEE Trans. Power Electron.*, vol. 30, no. 4, pp. 3164-3177, Apr. 2019.

[20] M. Abrehdari1, and M. Sarvi1, "Comprehensive sharing control strategy for input-series output-parallel connected modular DC–DC converters", *IET Power Electron*., vol. 12, no. 12, pp. 3105 - 3117, Dec. 2019.

[21] J. Shi, J. Luo, and X. He, "Common-duty-ratio control of input-series output-parallel connected phase-shift full-bridge DC–DC converter modules", *IEEE Trans. Power Electron.*, vol. 26, no. 11, pp. 3318 - 3329, Nov. 2011.

[22] F. Liu, G. Zhou, X. Ruan, S. Ji, Q. Zhao, and X. Zhang, "An input-series-output-parallel converter system exhibiting natural input voltage sharing and output-current sharing", *IEEE Trans. Ind. Electron.*, 2020, Early Access.

[23] L. Qu , D. Zhang , and B. Zhang, "Input voltage sharing control scheme for input series and output parallel connected DC–DC converters based on peak current control," *IEEE Trans. Ind. Electron.*, vol. 68, no. 1, pp. 429 - 439, Jan. 2019.

[24] H. Zhang, Y. Li, Z. Li, C. Zhao, F. Gao, Y. Hu, L. Luo, K. Luan, and P. Wang, "Model predictive control of input-series output-parallel dual active bridge converters based DC transformer", *IET Power Electron*., vol. 13, no. 6, pp. 1144 - 1152, Jun. 2020.

[25] J. Liu, J. Yang, J. Zhang, Z. Nan and Q. Zheng, "Voltage balance control based on dual active bridge DC/DC converters in a power electronic traction transformer", *IEEE Trans. Power Electron.*, vol. 33, no. 2, pp. 1696 - 1714, Feb. 2018.

[26] D. Sha, Z. Guo, and X. Liao, "Cross-feedback output-current-sharing control for input-series-output-parallel modular DC–DC converters," *IEEE Trans. Power Electron*., vol. 25, no. 11, pp. 2762 - 2771, Nov. 2010.

[27] L. Qu , D. Zhang and Z. Bao, "Output current-differential control scheme for input-series–output-parallel-connected modular DC–DC converters," *IEEE Trans. Power Electron.*, vol. 32, no. 7, pp. 5699 - 5711, Jul. 2017.

[28] W. Chen, G. Wang, X. Ruan, W. Jiang and W. Gu, "Wireless input-voltage-sharing control strategy for input-series output-parallel (ISOP) system based on positive output-voltage gradient method", *IEEE Trans. Power Electron.*, vol. 61, no. 11, pp. 6022-6030, Nov. 2014.

[29] G. Xu, D. Sha, and X. Liao, "Decentralized inverse-droop control for input-series–output-parallel DC–DC converters", *IEEE Trans. Power Electron.*, vol. 30, no. 9, pp. 4621-4625, Sept. 2015.

[30] W. Chen, and G. Wang, "Decentralized voltage-sharing control strategy for fully modular input-series–output-series system with improved

voltage regulation", *IEEE Trans. Ind. Electron.*, vol. 62, no. 5, pp. 2777 - 2787, May 2015.
[31] C. Luo and S. Huang, "Novel voltage balancing control strategy for dual-active-bridge input-series-output-parallel DC-DC converters", *IEEE Access*, vol. 8, pp. 103114-103123, Aug. 2020.
[32] T. Fang, L. Shen, W. He, and X. Ruan, "Distributed control and redundant technique to achieve superior reliability for fully modular input-series-output-parallel inverter system", *IEEE Trans. Power Electron.*, vol. 32, no. 1, pp. 723 - 735, Jan. 2017.
[33] P. Chaudhary, S. Samanta and P. Sensarma, "Input-series-output-parallel-connected buck rectifiers for high-voltage applications," *IEEE Trans. Ind. Electron.*, vol. 62, no. 1, pp. 193 - 202, Jan. 2015.
[34] W. Chen, X. Jiang, W. Cao, J. Zhao, W. Jiang, and L. Jiang, "A fully modular control strategy for input-series output-parallel (ISOP) inverter system based on positive output-voltage-amplitude gradientn", *IEEE Trans. Power Electron.*, vol. 33, no. 4, pp. 2878 - 2887, Apr. 2018.
[35] L. Shu, W. Chen and X. Jiang, "Decentralized control for fully modular input-series output-parallel (ISOP) inverter system based on the active power inverse-droop method", *IEEE Trans. Power Electron.*, vol. 33, no. 9, pp. 7521 - 7530, Sept. 2018.
[36] A. M. I. Mohamad and Y. A. R. I. Mohamed, "Investigation and enhancement of stability in grid-connected active DC distribution systems with high penetration level of dynamic loads", *IEEE Trans. Power Electron.*, vol. 34, no. 9, pp. 9170 - 9190, Apr. 2019.
[37] Y. Cai, J. Xu, P. Yang and G. Liu, "Design of double-line-frequency ripple controller for quasi-single-stage AC-DC converter with audio susceptibility model", *IEEE Trans. Ind. Electron.*, vol. 66, no. 12, pp. 9226-9237, Dec. 2019.
[38] X. Ruan, W. Chen, L. Cheng, C. K. Tse, H. Yan and T. Zhang, "Control strategy for input-series-output-parallel converters", *IEEE Trans. Ind. Electron.*, vol. 56, no. 4, pp. 1174-1185, Apr. 2009.

Yu Wang (M'19) was born in Guangdong, China, in 1984. He received the B.S. degree in Electronic Engineering from Nanchang Hangkong University, Nanchang, China, in 2007, the M.S. degree in Control Engineering from Guangxi University, Nanning, China, in 2010, and the Ph.D. degree in Power Electronics from South China University of Technology, Guangzhou, China, in 2015.

From 2015 to 2017, he worked as a Postdoctoral Researcher in Department of Electrical Engineering, Tsinghua University, Beijing, China. Since 2018, he becomes an Associate Professor in School of Automation, Guangdong University of Technology, Guangzhou, China. From December 2019 to December 2020, he was an ERCIM "Alain Bensoussan" Research Fellow in the Department of Electric Power Engineering, Norwegian University of Science and Technology, Trondheim, Norway.

Dr. Wang is a Member of IEEE and a Senior Member of China Power Supply Society. His current research interests include high-frequency power electronic solid-state transformer and flexible DC transmission and distribution systems.

Yuanpeng Guan was born in Hainan, China, in 1992. He received B.S. degree in Electrical Engineering from Huazhong University of Science and Technology, Wuhan, China, in 2014, the M.S. degree in Power Electronic from South China University of Technology, Guangzhou, China, in 2017, and the Ph.D. degree in Power Electronic from South China University of Technology, Guangzhou, China, in 2020.

He is currently an Associate Professor in the Energy Electricity Research Center, Jinan University, Zhuhai, China. His current research interests include grid-connected inverter and dual-active-bridge DC/DC converter.

Olav Bjarte Fosso (M'90–SM'06) is currently a Professor at the Department of Electric Power Engineering, Norwegian University of Science and Technology (NTNU), Trondheim, Norway. He has previously held positions as Scientific Advisor and Senior Research Scientist at SINTEF Energy Research, and Director of NTNUs Strategic Thematic Area Energy from September 2014 - September 2016. He has been Chairman of CIGRE SC C5 Electricity Markets and Regulation and Member of CIGRE Technical Committee (2008 – 2014). He has been expert evaluator in Horizon2020 and several science foundations, internationally. His research activities involve hydro scheduling, market integration of intermittent generation and signal analysis for study of power system's dynamics and stability.

Marta Molinas (M'94) received the Diploma degree in electromechanical engineering from the National University of Asuncion, Asuncion, Paraguay, in 1992, the Master of Engineering degree from Ryukyu University, Nishihara, Japan, in 1997, and the Doctor of Engineering degree from the Tokyo Institute of Technology, Tokyo, Japan, in 2000.

She was a Guest Researcher with the University of Padova, Padova, Italy, during 1998. From 2004 to 2007, she was a Postdoctoral Researcher with the Norwegian University of Science and Technology (NTNU), Trondheim, Norway, and from 2008 to 2014 she was a Professor with the Department of Electric Power Engineering at the same university. She is currently a Professor with the Department of Engineering Cybernetics, NTNU, Trondheim, Norway. Her research interests include stability of power electronics systems, harmonics, instantaneous frequency and non-stationary signals from the human and the machine.

Dr. Molinas is an Editor for the IEEE JOURNAL JESTPE, Associate Editor for IEEE PELS TRANSACTIONS and Editor of the IEEE TRANSACTIONS ON ENERGY CONVERSION. She has been an AdCom Member of the IEEE Power Electronics Society from 2009 to 2011.

Si-Zhe Chen was born in Shantou, China, in 1981. He received the B.Sc. in Mechatronic Engineering and the Ph.D. degree in Control Engineering from the South China University of Technology, Guangzhou, China, in 2005 and 2010, respectively.

He is currently an Associate Professor with the School of Automation, Guangdong University of Technology, Guangzhou, China. His current research interests include the control and power electronics technology in renewable energy systems.

Yun Zhang received the B.S. and M.S. degrees in Control Engineering from the Hunan University, Changsha, China, in 1982 and 1986, respectively, and the Ph. D. degree in Control Engineering from the South China University of Technology, Guangzhou, China, in 1998.

He is currently a Professor with the School of Automation, Guangdong University of Technology, Guangzhou, China. His current research interests include the intelligent control systems, signal processing and power electronics.